Annals of Telecommunications (2020) 75:641–653
https://doi.org/10.1007/s12243-020-00803-1

Quantum signal processing for quantum phase estimation: Fourier transform versus maximum likelihood approaches

François Chapeau-Blondeau[1] · Etienne Belin[1]

Received: 18 March 2020 / Accepted: 20 August 2020 / Published online: 5 September 2020

Abstract

The phase in quantum states is an essential information carrier for quantum telecommunications, signal processing, and computation. Quantum phase estimation is therefore a fundamental operation to extract and control useful information at the quantum level. Here, we analyze various approaches to quantum phase estimation, when a phase parameter characterizing a quantum process gets imprinted in a relative phase attached to a quantum state serving as a probe signal. The estimation approaches are based on standard concepts of signal processing (Fourier transform, maximum likelihood), yet operated in the quantum realm. We also exploit the Fisher information, both in its classical and its quantum forms, in order to assess the performance of each approach to quantum phase estimation. We demonstrate a possibility of enhanced estimation performance, inaccessible classically, which is obtained via optimized quantum entanglement. Beyond their significance to quantum phase estimation, the results illustrate how standard concepts of signal processing can contribute to the ongoing developments in quantum information and quantum technologies.

Keywords Quantum signal · Quantum phase · Quantum estimation · Quantum Fourier transform · Maximum likelihood · Fisher information

1 Introduction

Quantum methodologies and quantum technologies hold large potentialities for information processing, telecommunications, and computation [1]. Provably secure telecommunications, high-precision metrology, high-sensitivity sensing, quantum computers, and quantum networking represent diverse application areas, which are diversely advanced and currently under intense development, and where quantum approaches can offer decisive contributions for enhanced performance [2–8]. In this context, quantum states constitute information-carrying signals for quantum telecommunications, information processing, and computation. Quantum states are normalized state vectors defined on a complex Hilbert space, and they remain with unit norm throughout any valid quantum processing. Beyond its unit norm, the phase associated with a quantum state stands as an essential carrier for the information contained in a quantum state. The phase or relative phases in quantum states condition their properties of coherence, interference, and interaction, and determine their ability for information processing and computation [9, 10]. Quantum states when interacting with quantum processes or devices often experience an alteration in their phase; and such phase modification on quantum states in turn can serve as a probe to characterize or monitor quantum processes or devices [3, 4]. Quantum phase estimation from quantum states is therefore a fundamental operation to extract and control useful information at the quantum level. For instance, quantum phase estimation is essential to the functioning of quantum clocks, or for establishing high-precision frequency standards, or to high-sensitivity magnetometry [3, 4, 11, 12]. Quantum phase estimation is also an essential step of the Shor algorithm for factoring integers in polynomial complexity, with a significant bearing for cryptography and secure telecommunications [10, 13].

In this paper, we will analyze various approaches to quantum phase estimation, in the generic situation where a

✉ François Chapeau-Blondeau
f.chapeau@univ-angers.fr

Etienne Belin
etienne.belin@univ-angers.fr

[1] Laboratoire Angevin de Recherche en Ingénierie des Systèmes (LARIS), Université d'Angers, 62 avenue Notre Dame du Lac, 49000, Angers, France

phase parameter characterizing a quantum process or device gets imprinted in a relative phase attached to a quantum state serving as a probe signal. These estimation approaches will be based on standard concepts of signal processing—Fourier transform, maximum likelihood—yet operated in the quantum realm. We will also exploit the Fisher information, both in its classical and its quantum forms, in order to assess the performance of each approach examined for quantum phase estimation. The results carry relevance to quantum phase estimation; they also illustrate how standard concepts of signal processing apply to contribute to the ongoing developments in quantum information and quantum technologies, and in this way substantiate the capabilities of quantum signal processing.

2 Qubit phase

For the sake of definiteness, we will consider phase estimation from qubit states, although other quantum states can be handled in a similar way. The qubit or quantum bit [9] is a fundamental system of quantum information, which can be described by a state vector $|\psi\rangle$ belonging to a two-dimensional complex Hilbert space $\mathcal{H}_2$, and endowed with a unit squared norm $\langle\psi|\psi\rangle = 1$. When the space $\mathcal{H}_2$ is referred to the natural orthonormal basis $\{|0\rangle, |1\rangle\}$, the quantum state of a qubit can be any normalized superposition $|\psi\rangle = \alpha_0|0\rangle + \alpha_1|1\rangle \in \mathcal{H}_2$ with two complex coordinates satisfying $|\alpha_0|^2 + |\alpha_1|^2 = \langle\psi|\psi\rangle = 1$. A qubit for instance is a good model for a photon with its two states of polarization, or an electron with its two states of spin.

To get involved in a task of phase estimation, such a qubit state $|\psi\rangle$ is applied as an excitation signal to probe a quantum process or device represented by the unitary operator (any valid evolution of a closed quantum system is modeled by a unitary operator [9]):

$$\mathsf{U}_\xi = |0\rangle\langle 0| + e^{i2\pi\xi}|1\rangle\langle 1| = \begin{bmatrix} 1 & 0 \\ 0 & e^{i2\pi\xi} \end{bmatrix}, \tag{1}$$

characterized by a phase parameter $\xi \in [0, 1[$. The general state $|\psi\rangle = \alpha_0|0\rangle + \alpha_1|1\rangle$ of a qubit is affected by the process U_ξ of Eq. 1 according to:

$$\mathsf{U}_\xi|\psi\rangle = \alpha_0|0\rangle + e^{i2\pi\xi}\alpha_1|1\rangle, \tag{2}$$

inducing a phase shift of $2\pi\xi \in [0, 2\pi[$ between the two components of the qubit state. This represents for instance the fundamental operation taking place in an optical interferometer that, for a photon with its two states of polarization, would leave invariant a reference state $|0\rangle$, and would add a phase shift determined by $\xi \in [0, 1[$ on the other orthogonal state $|1\rangle$, as depicted in Fig. 1. Such an interferometer is a fundamental device of physics and metrology, which for instance recently served to the first observation of gravitational waves [14], and we are thus concerned here with interferometry at the ultimate level of individual photons.

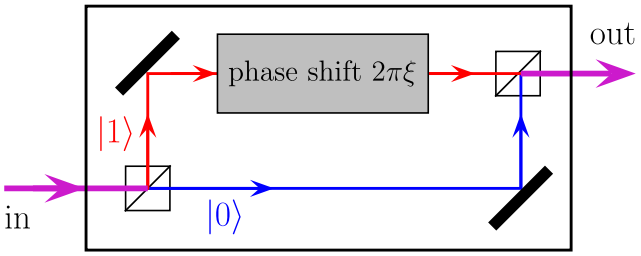

Fig. 1 Mach-Zehnder interferometer, featuring two polarizing beam splitters and two mirrors, to realize between the input (in) and output (out), a photonic implementation of the qubit transformation U_ξ of Eq. 1 with a phase shift determined by the parameter $\xi \in [0, 1[$ which is to be estimated

Any qubit unitary operator U has two complex unit-modulus eigenvalues of the form $e^{i\varphi_1}$ and $e^{i\varphi_2}$, associated with two orthogonal eigenstates. In this eigenbasis, U has the diagonal matrix form $\mathsf{U} = \mathrm{diag}[e^{i\varphi_1}, e^{i\varphi_2}]$, which can be factored as $\mathsf{U} = e^{i\varphi_1}\mathrm{diag}[1, e^{i(\varphi_2-\varphi_1)}]$. A global phase factor like $e^{i\varphi_1}$ affecting a quantum state $|\psi\rangle$ has no physically detectable effect, $|\psi\rangle$ and $e^{i\varphi_1}|\psi\rangle$ being two physically equivalent states [9]. So, U is equivalent to the unitary evolution by $\mathrm{diag}[1, e^{i(\varphi_2-\varphi_1)}]$. Consequently, by referring it to its eigenbasis, any qubit unitary operator can be put under the generic matrix form $\mathrm{diag}\left[1, e^{i2\pi\xi}\right]$ of Eq. 1 with $\varphi_2 - \varphi_1 = 2\pi\xi$. In the photonic implementation of Fig. 1, the eigenbasis is selected by rotating the beam splitters.

The phase shift $2\pi\xi \in [0, 2\pi[$ imprinted on the qubit state by U_ξ in Eq. 2 is determined by the phase parameter $\xi \in [0, 1[$ for which we use the term "phase" for convenience. For the interferometer of Fig. 1, such phase reflects a difference of optical paths in the device; in quantum magnetometry, the phase relates to the magnetic field enclosed by the device. The task is then to efficiently estimate the phase $\xi \in [0, 1[$ characterizing the quantum process U_ξ of Eq. 1. The process U_ξ is not directly measurable, but only through the alteration it produces on quantum states like $|\psi\rangle$ in Eq. 2. Qubit states will therefore be used to constitute a probe or excitation signal applied to the process U_ξ of Eq. 1. The phase alteration according to Eq. 2 resulting on such a quantum state will be used to estimate the phase parameter ξ. From the viewpoint of signals and systems theory, this can be seen as a task of parameter estimation performed on a probe signal for system identification. For probing the process U_ξ of Eq. 1, it can be profitable to assemble N qubits to form a composite signal of N qubits whose joint quantum state belongs to the tensor-product space $\mathcal{H}_2^{\otimes N}$ with dimension 2^N referred to the orthonormal basis $\{|0\cdots 0\rangle, |0\cdots 1\rangle, \cdots, |1\cdots 1\rangle\}$ where each of the 2^N basis vectors $|j\rangle$ is identified by a

binary word of N bits. Common notations in use [9] for tensor-product quantum states are $|\cdot\rangle\cdots|\cdot\rangle \equiv |\cdot\rangle\otimes\cdots\otimes|\cdot\rangle \equiv |\cdots\rangle$.

For estimating the phase ξ from a multiple-qubit input probe signal, there exists an efficient approach that exploits the quantum Fourier transform. We will now briefly review the basic properties of the quantum Fourier transform that will serve for quantum phase estimation.

3 Quantum Fourier transform

The quantum Fourier transform is conveniently defined as a change of orthonormal basis (instead of a change or coordinates which may be more common in classical signal processing) for the representation of quantum states. A quantum system with an L-dimensional complex Hilbert space $\mathcal{H}_L$ is referred to the natural orthonormal basis formed by the set of L state vectors $|j\rangle \in \{|0\rangle, |1\rangle, \ldots |L-1\rangle\}$. The quantum Fourier transform is then defined [9] as the unitary change of basis:

$$|j\rangle \longmapsto |\widetilde{j}\,\rangle = \frac{1}{\sqrt{L}}\sum_{k=0}^{L-1}\exp\Big(i2\pi\frac{jk}{L}\Big)|k\rangle\,, \qquad \text{for } j=0,\ldots L-1\,, \tag{3}$$

which delivers the set of L vectors $\{|\widetilde{j}\,\rangle\} = \{|\widetilde{0}\rangle, |\widetilde{1}\rangle, \ldots |\widetilde{L-1}\rangle\}$ forming another orthonormal (Fourier) basis of $\mathcal{H}_L$. In operator notation, the two bases are related through $|\widetilde{j}\,\rangle = \mathsf{U_F}|j\rangle$ via the unitary operator $\mathsf{U_F}$ represented by the $L\times L$ symmetric matrix with generic term $\big[\exp(i2\pi jk/L)\big]/\sqrt{L}$ in the natural basis.

The inverse Fourier transform is defined by the reverse change of basis inverting the transformation of Eq. 3 and transforming the Fourier basis $\{|\widetilde{j}\,\rangle\} = \{|\widetilde{0}\rangle, |\widetilde{1}\rangle, \ldots |\widetilde{L-1}\rangle\}$ back into the original natural basis $\{|j\rangle\} = \{|0\rangle, |1\rangle, \ldots |L-1\rangle\}$, and reading:

$$|\widetilde{j}\,\rangle \longmapsto |j\rangle = \frac{1}{\sqrt{L}}\sum_{k=0}^{L-1}\exp\Big(-i2\pi\frac{jk}{L}\Big)|\widetilde{k}\,\rangle\,, \qquad \text{for } j=0,\ldots L-1\,, \tag{4}$$

or equivalently $|j\rangle = \mathsf{U_F^\dagger}|\widetilde{j}\,\rangle$ since by unitarity $\mathsf{U_F^{-1}} = \mathsf{U_F^\dagger}$ the conjugate transpose.

The quantum Fourier transform of Eq. 3 and its inverse of Eq. 4 are related to the original orthonormal basis denoted $\{|0\rangle, |1\rangle, \ldots |L-1\rangle\}$ here. Yet, in principle, a quantum Fourier transform can be defined equivalently from any orthonormal basis of a working Hilbert space.

Equation 3 can also be written as $|\widetilde{j}\,\rangle = L^{-1/2}\sum_{k=0}^{L-1}\exp(i2\pi\xi_j k)|k\rangle$, with $\xi_j = j/L \in [0,1[$ and the phase $2\pi\xi_j \in [0, 2\pi[$. This shows that the transformed state $|\widetilde{j}\,\rangle$ is a quantum state constructed as a superposition of all the basis states $|k\rangle$ of the natural basis, each one weighted by a complex phase factor $\exp(i2\pi\xi_j k)$ involving the k-th multiple of the fixed phase $2\pi\xi_j$. This provides the ground for the application of the quantum Fourier transform to quantum phase estimation. By probing a quantum process characterized by a dephasing action via a phase like ξ_j, so as to excite all the multiples $\xi_j k$ gathered in a response signal like $|\widetilde{j}\,\rangle$, one will have the faculty, by inverse Fourier transform on the probing state $|\widetilde{j}\,\rangle$ according to Eq. 4, of obtaining the index j that identifies the unknown phase ξ_j. This Fourier-based approach to quantum phase estimation is now addressed in more detail.

4 Fourier transform quantum phase estimation

Application of the quantum Fourier transform to quantum phase estimation is commonly originated in the work of Kitaev [15], and has been further analyzed in [9, 16, 17]. Extensions have been proposed to obtain enhanced estimation efficiency [18–21], especially by exploiting the specifically quantum property of entanglement.

Here, we consider the Fourier-based method in its variant presented in [22] for phase estimation on a qubit process as in Eq. 1, and extended in [23] to phase estimation on an arbitrary quantum process. As original complements to [22, 23], here we will assess the performance of the Fourier-based estimation of [22, 23] by means of the Fisher information establishing the overall maximal efficiency; and we will also compare it with a direct maximum likelihood approach for quantum phase estimation; with the presentation of the results organized in a consistent (quantum) signal-processing perspective.

For efficient estimation, we consider the $(N-1)$-qubit excitation signal defined by the joint state, denoted $|\bar{k}\,\rangle$, for integer $k = 0$ to $N-1$, formed with the k first qubits placed in state $|1\rangle$ and the remaining qubits placed in state $|0\rangle$, according to:

$$|\bar{k}\,\rangle = \overbrace{|0\rangle\cdots|0\rangle}^{N-1}\underbrace{|1\rangle\cdots|1\rangle}_{k} = \big|\overbrace{0\cdots0}^{N-1}\underbrace{1\cdots1}_{k}\big\rangle\,. \tag{5}$$

The set of N states $\{|\bar{k}\,\rangle\}$, for $k = 0$ to $N-1$, forms an orthonormal basis for the N-dimensional subspace $\mathcal{H}'_N$ of the 2^{N-1}-dimensional Hilbert space $\mathcal{H}_2^{\otimes(N-1)}$ of the $N-1$ qubits. All the operations that are going to take place will maintain the quantum states in the subspace $\mathcal{H}'_N$, which is established in this way as the working Hilbert space.

The $N-1$ qubits in state $|\bar{k}\,\rangle \in \mathcal{H}'_N$ can act as an excitation signal to the process U_ξ of Eq. 1, as depicted in Fig. 2. Each of the $N-1$ input qubits is individually physically materialized, and it can therefore be applied

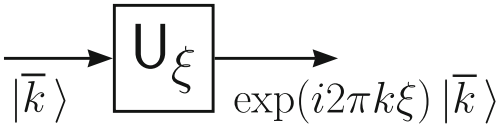

Fig. 2 The excitation signal $|\bar{k}\rangle$ of Eq. 5 with its $N-1$ qubits sequentially applied at the input of the quantum gate materializing the process U_ξ of Eq. 1, induces the output response signal $\exp(i2\pi k\xi)|\bar{k}\rangle$ of Eq. 6

sequentially, one after the other, to the quantum gate materializing the process U_ξ of Eq. 1. For example, this would consist in sending $N-1$ photons, one by one, across the interferometer of Fig. 1.

According to the operation of the process U_ξ defined by Eq. 2, the two basis states of the qubit transform as $|0\rangle \mapsto \mathsf{U}_\xi|0\rangle = |0\rangle$ and $|1\rangle \mapsto \mathsf{U}_\xi|1\rangle = \exp(i2\pi\xi)|1\rangle$. Consequently, the $(N-1)$-qubit state $|\bar{k}\rangle$ of Eq. 5 gets transformed as:

$$|\bar{k}\rangle \longmapsto \mathsf{U}_\xi^{\otimes(N-1)}|\bar{k}\rangle = \exp(i2\pi k\xi)|\bar{k}\rangle\ . \tag{6}$$

A specially useful possibility is that the $N-1$ input qubits can be prepared in an arbitrary superposition of the N basis states $\{|\bar{k}\rangle\}$ under the form:

$$|\psi_{\rm in}\rangle = \sum_{k=0}^{N-1} a_k|\bar{k}\rangle\ , \tag{7}$$

with the complex coefficients $a_k \in \mathbb{C}$ normalized by $\sum_{k=0}^{N-1}|a_k|^2 = 1$. This specific form of the excitation signal $|\psi_{\rm in}\rangle$ in Eq. 7 was introduced in [22]. It bears some similarities with the excitation signal used in [19], but it also differs in some places. Especially, compared with that of [19], the excitation of Eq. 7 involves a different superposition, with a smaller number of basis states, and with a form in Eq. 7 that made it possible to analyze the impact of quantum noise on the estimation efficiency as accomplished in [22, 23]. Moreover, for the estimation based on the excitation signal of Eq. 7, an assessment of the performance will be worked out in Sections 5–7, which is new here and not contained in [22, 23].

The basis states $|\bar{k}\rangle$ of Eq. 5 are separable (factorizable) states of $N-1$ qubits. However, for arbitrary coefficients a_k, the superposition $|\psi_{\rm in}\rangle$ of Eq. 7 generally forms an entangled state of the $N-1$ qubits, not factorizable as tensor products of one-qubit states. And we shall see later on that exploiting this entanglement will be an important feature for enhanced performance in estimation. The input excitation signal $|\psi_{\rm in}\rangle \in \mathcal{H}'_N$ in Eq. 7, by linearity applying on Eq. 6, induces in the setting of Fig. 2 the output response:

$$|\widetilde{\psi}_\xi\rangle = \mathsf{U}_\xi^{\otimes(N-1)}|\psi_{\rm in}\rangle = \sum_{k=0}^{N-1} a_k \exp\left(i2\pi\frac{j_\xi k}{N}\right)|\bar{k}\rangle \tag{8}$$

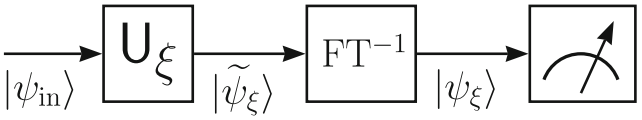

Fig. 3 An excitation signal $|\psi_{\rm in}\rangle$ formed by $N-1$ input qubits prepared in the orthonormal basis $\{|\bar{k}\rangle\}$ of $\mathcal{H}'_N$ as the superposed state of Eq. 7 is applied to the quantum gate materializing the process U_ξ of Eq. 1, which responds by producing the ξ-dependent probing signal $|\widetilde{\psi}_\xi\rangle$ of Eq. 8, which is inverse-Fourier-transformed to deliver the signal $|\psi_\xi\rangle = \mathsf{U}_{\mathsf{F}}^\dagger|\widetilde{\psi}_\xi\rangle$ of Eq. 9, which is finally measured in the basis $\{|\bar{k}\rangle\}$, in order to estimate the unknown phase ξ

with $j_\xi = N\xi$. With the state $|\widetilde{\psi}_\xi\rangle$ of Eq. 8, constituting the ξ-dependent response or probing signal, we are coming close to the superposed state envisaged in the last paragraph of Section 3 above.

An inverse Fourier transform referred to the orthonormal basis $\{|\bar{k}\rangle\}$ of the working Hilbert space $\mathcal{H}'_N$ is performed on the probing signal $|\widetilde{\psi}_\xi\rangle$, according to Eq. 4, to obtain:

$$\mathsf{U}_{\mathsf{F}}^\dagger|\widetilde{\psi}_\xi\rangle = |\psi_\xi\rangle = \sum_{j=0}^{N-1} a'_j|\bar{\jmath}\rangle\ , \tag{9}$$

with the coefficients

$$a'_j = \frac{1}{\sqrt{N}}\sum_{k=0}^{N-1} a_k \exp\left(i2\pi\frac{(j_\xi - j)k}{N}\right)\ , \tag{10}$$

for $j = 0$ to $N-1$. The ξ-dependent state $|\psi_\xi\rangle \in \mathcal{H}'_N$ of Eq. 9 is then measured in the orthonormal basis $\{|\bar{k}\rangle\}$ of $\mathcal{H}'_N$ in order to estimate ξ.

The whole procedure, from excitation to measurement, performs the feed-forward signal-processing pipeline depicted in Fig. 3, where the input signal $|\psi_{\rm in}\rangle$ of Eq. 7 is prepared in the basis $\{|\bar{k}\rangle\}$ and the output signal $|\psi_\xi\rangle$ of Eq. 9 is measured in the same basis $\{|\bar{k}\rangle\}$.

It can be noted that measuring the transformed state $|\psi_\xi\rangle = \mathsf{U}_{\mathsf{F}}^\dagger|\widetilde{\psi}_\xi\rangle$ in the orthonormal basis $\{|\bar{k}\rangle\}$ would be equivalent to measuring the state $|\widetilde{\psi}_\xi\rangle$ in the transformed basis $\{\mathsf{U}_{\mathsf{F}}|\bar{k}\rangle\}$, except for the post-measurement state. Also, beyond the standard projective (von Neumann) quantum measurement in the orthonormal basis $\{|\bar{k}\rangle\}$, one could envisage a generalized quantum measurement [9], forming an extension to von Neumann measurements which amounts to measuring the quantum states in an enlarged Hilbert space. Such generalized measurements are usually more complicated to implement practically and to handle theoretically. They may or may not offer some added capability for enhanced performance. We will come back to them later in the sequel, showing significant situations where they are not profitable to maximize the performance. We now proceed with the analysis of the Fourier-based estimation strategy of Fig. 3, preparing and measuring the states in the basis $\{|\bar{k}\rangle\}$.

According to quantum theory and the Born rule [9], the measurement of the quantum state $|\psi_\xi\rangle$ of Eq. 9 in the basis $\{|\overline{k}\,\rangle\}$, generally projects on the basis state $|\overline{j}\,\rangle$ and delivers the integer j with probability $P_j = |a'_j|^2$, for $j = 0$ to $N-1$.

In the case of a uniform superposition with all $a_k = 1/\sqrt{N}$ in Eq. 7, and an unknown phase $\xi \in [0, 1[$ that would yield $j_\xi = N\xi = j_0$ precisely an integer $j_0 \in [0, N[$, one would have $a'_j = \delta_{jj_0}$ and $|\psi_\xi\rangle = |\overline{j}_0\rangle$ in Eq. 9. The measurement of $|\psi_\xi\rangle$ would then deliver j_0 exactly, and therefrom the estimator $\widehat{\xi} = j_0/N$ would recover the exact phase $\widehat{\xi} = \xi$.

In the generic situation of a phase ξ with $j_\xi = N\xi$ non-integer, the same protocol of Fig. 3 is employed. The probability distribution $P_j = |a'_j|^2$ takes the form of a sharp peak (of width $\sim 1/N$) around an integer j very close to j_ξ. The measurement of the state $|\psi_\xi\rangle \in \mathcal{H}'_N$ of Eq. 9 then returns such integer j from which the estimator $\widehat{\xi} = j/N$ allows one to recover the unknown phase ξ with a good precision at $1/N$ resolution. For any given (measured) j, the probability $P_j = |a'_j|^2$ resulting from Eq. 10 when seen as a function of ξ represents the likelihood, and maximized by $\xi = j/N$ it establishes $\widehat{\xi} = j/N$ as the maximum likelihood estimator. It can be noted that since the basis states $|\overline{k}\,\rangle$ of Eq. 5 are separable (factorizable) states, measurement in the projective basis $\{|\overline{k}\,\rangle\}$ of the state $|\psi_\xi\rangle$ with $N-1$ qubits can in practice be carried out by measuring each of the $N-1$ qubits separately in the basis $\{|0\rangle, |1\rangle\}$, and then counting the number j of qubits measured (projected) in $|1\rangle$. This applies even when the state $|\psi_\xi\rangle$ is entangled, since each of the $N-1$ qubits remains physically accessible individually.

This estimation protocol is characterized by a mean-squared error:

$$e^2(\widehat{\xi}\,) = \left\langle \left(\widehat{\xi} - \xi\right)^2 \right\rangle = \sum_{j=0}^{N-1} \left(\frac{j}{N} - \xi\right)^2 P_j \,. \tag{11}$$

Detailed derivations for the mean-squared estimation error are developed in various configurations in [23].

In the case of a uniform superposition $a_k = 1/\sqrt{N}$ in Eq. 7, the sum of Eq. 10 can be explicitly carried out to give

$$a'_j = \frac{1}{N} \frac{\sin\left[\pi(j_\xi - j)\right]}{\sin\left[\pi(j_\xi - j)/N\right]} \exp\left[i\pi \frac{N-1}{N}(j_\xi - j)\right] \,. \tag{12}$$

From Eq. 12, with the probability $P_j = |a'_j|^2$ placed in Eq. 11, it can be found [23] that in the regime of small error at large N, the mean-squared estimation error of Eq. 11 follows as:

$$e^2(\widehat{\xi}\,) = \frac{1}{\pi^2 N} \sin^2(\pi N \xi) \,. \tag{13}$$

From Eq. 13 is recovered the vanishing estimation error expected when $N\xi = j_0$ precisely an integer. Otherwise, in the generic case, Eq. 13 leads to a mean-squared estimation error evolving as $e^2(\widetilde{\xi}\,) \sim 1/N$, known as the shot-noise or standard scaling of the error [11]. This is the same standard scaling of the error that is found in the original Kitaev approach to Fourier-based quantum phase estimation [9, 15, 16]. This is also the same mean-squared estimation error in $1/N$ that can be expected in classical statistical estimation from $\sim N$ evaluations of the process to be estimated. Quantum physics however allows us to do better, to reach a performance inaccessible classically.

The input superposition $|\psi_{\rm in}\rangle$ of Eq. 7 usually represents an entangled (non-factorizable) quantum state for the $N-1$ qubits. Beyond the uniform $a_k = 1/\sqrt{N}$ in Eq. 7 associated with the performance of Eq. 13, it is possible to seek to optimally entangle the $N-1$ input qubits in Eq. 7. The mean-squared estimation error of Eq. 11 can be evaluated with arbitrary coefficients a_k in Eq. 7, which are then optimized to minimize the error. This is accomplished in [23] to find the optimal coefficients:

$$a_k = \sqrt{\frac{2}{N}} \sin\left(\pi \frac{k}{N}\right) \,, \quad k = 0, 1, \cdots N-1. \tag{14}$$

These optimal coefficients a_k of Eq. 14 can then be placed in Eq. 10, and the resulting sum can be explicitly evaluated to give:

$$a'_j = \frac{1}{N\sqrt{2}} \frac{\sin(\pi/N)}{\cos\left[2\pi(j_\xi - j)/N\right] - \cos(\pi/N)} \left(1 + \exp\left[i2\pi(j_\xi - j)\right]\right) \,. \tag{15}$$

From Eq. 15, with the probability $P_j = |a'_j|^2$ placed in Eq. 11, it is found [23] that in the regime of small error at large N, the optimal coefficients a_k of Eq. 14 achieve in Eq. 11 the minimal mean-squared error:

$$e^2(\widehat{\xi}\,) = \frac{1}{\pi^2} \sin^2\left(\frac{\pi}{2N}\right) \,, \tag{16}$$

instead of Eq. 13 with the uniform a_k's. The estimation error of Eq. 16 at large N is also $e^2(\widehat{\xi}\,) \approx 1/(4N^2)$, instead of a $1/N$ evolution from Eq. 13. With the optimal coefficients a_k of Eq. 14, the probability distribution $P_j = |a'_j|^2$ of the measurement results from Eq. 15 gets more peaked around the true value to be estimated, as illustrated in Fig. 4, whence a smaller mean-squared estimation error.

This is the striking benefit that can be obtained from an optimally entangled input superposition in $|\psi_{\rm in}\rangle$ of Eq. 7. With $\sim N$ evaluations of the process U_ξ to be estimated, the uniform superposition in $|\psi_{\rm in}\rangle$ achieves with Eq. 13 a mean-squared error evolving as $1/N$. By contrast, for $|\psi_{\rm in}\rangle$ the nonuniform optimal superposition of Eq. 14 is able to achieve a much reduced mean-squared estimation error evolving as $1/N^2$. This is known as the Heisenberg scaling of the error [8, 11, 24, 25], and constitutes a specifically quantum improvement, with no classical equivalent, obtained here by an optimally entangled excitation signal in Eq. 7. This Heisenberg

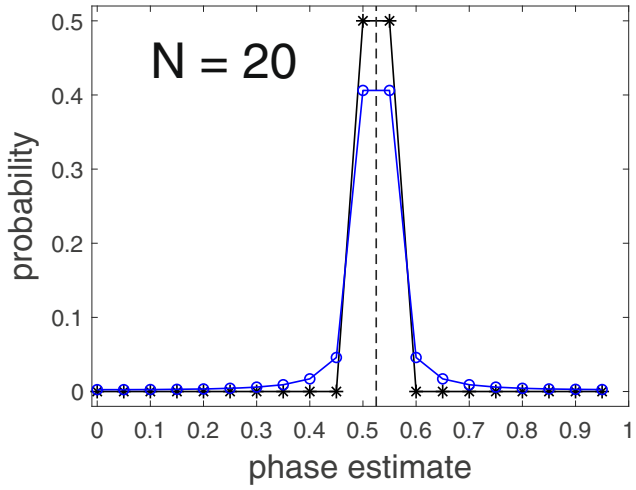

Fig. 4 The probability $\Pr(\widehat{\xi} = j/N) = P_j = |a'_j|^2$ for the estimate $\widehat{\xi}$ of the phase in abscissa, as it results: (∘) from Eq. 12 with the non-optimal uniform superposition $a_k = 1/\sqrt{N}$, or (∗) from Eq. 15 with the optimal input superposition of Eq. 14. The size $N = 20$. The true value of the phase to be estimated is $\xi = 0.5 + 0.5/N$ shown by the vertical dotted line

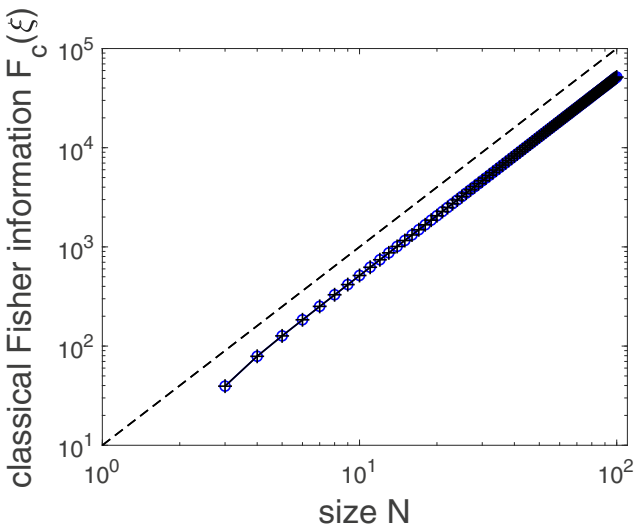

Fig. 5 Classical Fisher information $F_c(\xi)$ from Eq. 18, as a function of the size N conditioning the $(N-1)$-qubit state used as an excitation signal with the optimal coefficients a_k of Eqs. 14 and 15, for estimation of the phase ξ, with (∘) for $\xi = 0.5+0.5/N$, and (+) for $\xi = \sqrt{2}/3 \approx 0.471$. The dashed diagonal with slope 2 materializes the evolution as N^2

enhanced scaling of the efficiency in Fourier-based quantum phase estimation was also obtained in [18, 19] with differing approaches, but it was not present in the original approach by Kitaev [9, 15, 16].

As mentioned earlier, the Fourier-based estimation exploiting the entangled excitation signal of Eq. 7 was first introduced in [22] and later extended in [23]. We will now work out, throughout Sections 5 to 7, an evaluation and a confrontation of the estimation performance, which are new here and not contained in [22, 23].

5 Classical Fisher information

After inverse Fourier transform of the probing state $|\widetilde{\psi}_\xi\rangle$ of Eq. 8, measurement of the quantum state $|\psi_\xi\rangle$ of Eq. 9 delivers an integer $j \in [0, N-1]$ having the status of a classical random variable, with a probability distribution $P_j = |a'_j|^2$, for $j = 0$ to $N-1$, dependent upon the unknown phase parameter ξ to be estimated. From the value j delivered by the measurement, it is known from classical estimation theory [26, 27], that any estimator $\widehat{\xi}$ for ξ is endowed with a mean-squared error $e^2(\widehat{\xi}) = \langle(\widehat{\xi} - \xi)^2\rangle$ which is lower bounded by the Cramér-Rao bound involving the reciprocal of the classical Fisher information $F_c(\xi)$. In this respect, higher Fisher information $F_c(\xi)$ generally entails higher efficiency in estimation. We want now to evaluate the Fisher information $F_c(\xi)$ for an assessment of the performance of the Fourier-based approach to quantum phase estimation described in Section 4.

From the ξ-dependent probability distribution P_j, the classical Fisher information $F_c(\xi)$ is defined [26, 27] as the expectation:

$$F_c(\xi) = \Big\langle \big[\partial_\xi \ln(P_j)\big]^2 \Big\rangle = \sum_{j=0}^{N-1} \frac{1}{P_j} \left(\partial_\xi P_j\right)^2 \ , \tag{17}$$

with $\partial_\xi \cdot = \partial \cdot / \partial_\xi$ the derivative relative to ξ. Since here $P_j = |a'_j|^2$, one also has:

$$F_c(\xi) = 4 \sum_{j=0}^{N-1} \Big(\partial_\xi |a'_j|\Big)^2 \ . \tag{18}$$

With the coefficients a'_j given in Eq. 12 or in Eq. 15, the differentiation $\partial_\xi |a'_j|$ can be accomplished analytically. The final sum over j resulting in Eq. 18 remains difficult to evaluate analytically, yet its computation can be readily performed numerically. This allows us to obtain the Fisher information $F_c(\xi)$ and analyze its behavior, especially in relation to the Heisenberg-enhanced mean-squared estimation error of Eq. 16 evolving as $1/N^2$. Figure 5 displays the evolution of the Fisher information $F_c(\xi)$ from Eq. 18, corresponding to an excitation signal with the optimal coefficients a_k of Eqs. 14 and 15.

The evolutions of Fig. 5 show a classical Fisher information $F_c(\xi)$ in Eq. 18 which presents no significant dependence on the value of the unknown phase ξ to be estimated. Such a parameter-independent Fisher information $F_c(\xi)$ in Fig. 5 is an interesting property, not always obtained in parameter estimation, expressing here a uniform performance assessed by $F_c(\xi)$ which stays the

same for any range of the parameter ξ to be estimated. Such an invariance of $F_c(\xi)$ with ξ here can be explained as follows. According to the expression of a'_j from Eq. 15, for $F_c(\xi)$ in Eq. 18, the sum over j applies to a function $\left(\partial_\xi |a'_j|\right)^2$ that depends on j only through $2\pi(j_\xi - j)/N = 2\pi(\xi - j/N)$, and moreover in a way that makes $\left(\partial_\xi |a'_j|\right)^2$ (like a'_j) a periodic function in j with period N. At large N, the step $1/N$ of the sum in Eq. 18 gets finer and it can be approximated by an integral over the continuous variable $u = \xi - j/N$ applying to a periodic function in u of period 1, that, when integrated over one period with $u \in [0, 1[$, leaves no dependence in ξ of the result, since ξ acts as an irrelevant origin for the integration over one period, delivering in this way a ξ-independent $F_c(\xi)$. Although this argument applies at large N, we observe via numerical evaluation of $F_c(\xi)$ that such quasi-independence with ξ is present also at small N. This is confirmed by many more (exact numerical) evaluations of $F_c(\xi)$ at different values of ξ complementing those shown in Fig. 5.

Another significant property shown in Fig. 5 is that the Fisher information $F_c(\xi)$ resulting in Eq. 18 increases as N^2 with the size N controlling the dimension of the excitation signal $|\psi_{\text{in}}\rangle$ of Eq. 7 optimally entangled via Eqs. 14 and 15. This matches the $1/N^2$ evolution of the mean-squared estimation error $e^2(\widehat{\xi})$ obtained in Eq. 16 in the optimal configuration of Eqs. 14 and 15. Such an evolution as $F_c(\xi) \sim N^2$ is unusual for the Fisher information. Classically, in statistical estimation, with a number $\sim N$ of independent measurements or evaluations of the process to be estimated, an evolution as $F_c(\xi) \sim N$ ensues for the Fisher information. In such classical context, when correlation exists between the N data points, this usually corresponds to redundancy among them, which together carry less original information about the unknown parameter, this tending to reduce the Fisher information. So classically, there is usually no correlation pattern in the data known to enhance the Fisher information from a variation as $\sim N$ (at independence) to a variation as $\sim N^2$. By contrast, in the quantum domain, the variation $F_c(\xi) \sim N^2$ of the Fisher information is observed. This occurs in the presence of an excitation signal $|\psi_{\text{in}}\rangle$ of Eq. 7, of size controlled by the dimension N, incorporating a specific type of correlation under the form of an optimal quantum entanglement according to Eqs. 14 and 15. This is another manifestation of the specific character of the correlation realized by quantum entanglement, which can entail properties and performance inaccessible classically.

Beyond their variations controlled by N^2, it is also interesting to confront quantitatively the Fisher information $F_c(\xi)$ of Fig. 5 and the mean-squared estimation error $e^2(\widehat{\xi})$ of Eq. 16. In the conditions of Fig. 5, such confrontation is performed in Fig. 6.

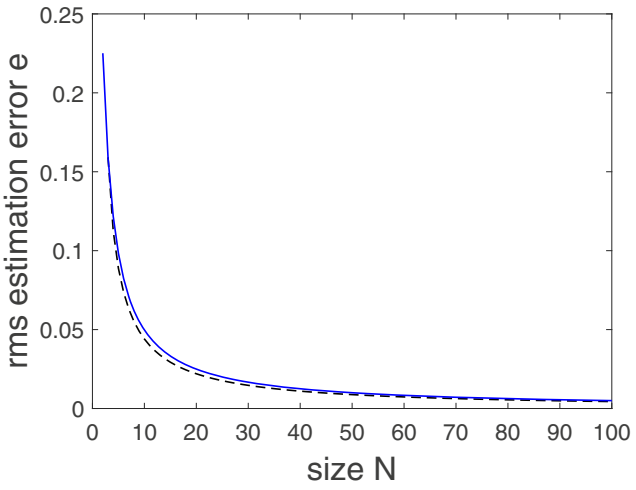

Fig. 6 Root-mean-squared estimation error $e(\widehat{\xi})$ of Eq. 16 (solid line) compared to $1/\sqrt{F_c(\xi)}$ (dashed line) with $F_c(\xi)$ the classical Fisher information of Fig. 5 (+), as a function of the size N controlling the dimension of the probing signal

In Fig. 6, the root-mean-squared (rms) estimation error $e(\widehat{\xi})$ from Eq. 16 is found just slightly above the bound $1/\sqrt{F_c(\xi)}$. The rms error $e(\widehat{\xi})$ in Fig. 6 is always below a factor of 1.14 from $1/\sqrt{F_c(\xi)}$. The bound $1/\sqrt{F_c(\xi)}$ is the asymptotic lower bound that can be expected, according to the Cramér-Rao inequality [26, 27], for the rms error of the maximum likelihood estimator at large N, which is an efficient estimator in this regime. The small departure in Fig. 6 between the rms error $e(\widehat{\xi})$ and the bound $1/\sqrt{F_c(\xi)}$ includes a small bias of the estimator $\widehat{\xi} = j/N$ which vanishes as $1/N$. The results of Fig. 6 show that the Fourier-based estimator $\widehat{\xi}$ optimized according to Eqs. 14–16 achieves an rms estimation error $e(\widehat{\xi})$ very close (barely above) the lower bound $1/\sqrt{F_c(\xi)}$ for any N.

In this respect, in the estimation protocol of Fig. 3, with the excitation signal $|\psi_{\text{in}}\rangle$ of Eq. 7 optimized via Eq. 14, when the probing signal $|\widetilde{\psi}_\xi\rangle$ of Eq. 8 is inverse-Fourier-transformed to produce the signal $|\psi_\xi\rangle = \mathsf{U}_{\mathsf{F}}^\dagger |\widetilde{\psi}_\xi\rangle$ of Eq. 9, based on the data obtained by measuring $|\psi_\xi\rangle$, the estimator $\widehat{\xi}$ achieving the mean-squared error $e^2(\widehat{\xi})$ of Eq. 16 is quasi-optimal, as it almost reaches the minimal conceivable error for any size N.

In the quantum context, there remains an issue that should be examined, regarding efficient estimation of the quantum phase. The classical Fisher information $F_c(\xi)$ of Eqs. 17 and 18 is specifically tied to the probability distribution $P_j = |a'_j|^2$ resulting from measuring the quantum state $|\psi_\xi\rangle$ of Eq. 9 via a projective measurement in the orthonormal basis $\{|\bar{k}\rangle\}$ of $\mathcal{H}'_N$. One could wonder whether a larger Fisher information $F_c(\xi)$ could be reached, based on another distribution of probability, resulting from another protocol of quantum measurement. Accordingly,

one could think of measuring another state related to the probing signal $|\widetilde{\psi}_\xi\rangle$ of Eq. 8, but differing from the inverse-Fourier-transformed state $|\psi_\xi\rangle$; and with a measurement differing from the projective measurement in the basis $\{|\bar{k}\rangle\}$. The quantum Fisher information is a notion to handle this issue.

6 Quantum Fisher information

For a quantum state $|\phi_\xi\rangle$ bearing dependence on a parameter ξ, with the differentiated state $\partial_\xi|\phi_\xi\rangle \equiv |\partial_\xi\phi_\xi\rangle$, the quantum Fisher information [28–31] is defined as the non-negative (real) scalar:

$$F_q(\xi) = 4\Big(\langle\partial_\xi\phi_\xi|\partial_\xi\phi_\xi\rangle + \langle\partial_\xi\phi_\xi|\phi_\xi\rangle^2\Big) \,. \tag{19}$$

The quantum Fisher information $F_q(\xi)$ is intrinsic to the relationship between the quantum state $|\phi_\xi\rangle$ and the parameter ξ. It does not refer to any particular quantum measurement performed on $|\phi_\xi\rangle$ for estimating ξ. By contrast, the classical Fisher information $F_c(\xi)$, as in Eqs. 17 and 18, is specifically tied to particular quantum measurement, via the probability distribution of the measurement results. The usefulness of the quantum Fisher information $F_q(\xi)$ is that it can be shown [28–31] that it provides an upper bound to the classical Fisher information $F_c(\xi)$ attached to any conceivable quantum measurement of the state $|\phi_\xi\rangle$, i.e.:

$$F_c(\xi) \le F_q(\xi) \,. \tag{20}$$

The inequality of Eq. 20 concerns any standard projective (von Neumann) quantum measurement, which consists in projecting an N-dimensional state $|\phi_\xi\rangle \in \mathcal{H}_N$ in an arbitrary orthonormal (projective) basis of $\mathcal{H}_N$. Changing the projective basis of $\mathcal{H}_N$ will change the probability distribution of the N measurement results, and hence will change the classical Fisher information $F_c(\xi)$, however always limited by Eq. 20. The inequality of Eq. 20 concerns also generalized quantum measurements [9], which consists in first coupling the state $|\phi_\xi\rangle$ to another quantum state (part of the measuring apparatus) so as to obtain a composite state of a larger dimension, whose projective measurement will deliver a number (usually) larger than N of measurement results for $|\phi_\xi\rangle$. These measurement results will also come with their probability distribution, to determine a classical Fisher information $F_c(\xi)$ in the usual way, which also is always limited by Eq. 20.

As a consequence of Eq. 20, in practice, if a quantum measurement is found that achieves $F_c(\xi) = F_q(\xi)$, then it is guaranteed that in this respect it is the most efficient measurement, and no other measurement could reach a higher classical Fisher information $F_c(\xi)$. However, the upper bound formed by the quantum Fisher information $F_q(\xi)$ in Eq. 20 does not generally stand as an achievable upper bound. Situations may exist with no definite (and parameter-independent as it should) quantum measurement able to achieve $F_c(\xi) = F_q(\xi)$, even by considering the broader class of generalized measurements.

In addition, the quantum Fisher information $F_q(\xi)$ of Eq. 19 is invariant under any ξ-independent unitary transformation U applied to the state $|\phi_\xi\rangle$, by virtue of $\mathsf{U}^\dagger\mathsf{U} = \mathrm{I}$ the identity operator.

Now for the present study of quantum phase estimation, it is meaningful to evaluate the quantum Fisher information $F_q(\xi)$ attached to the measured state $|\psi_\xi\rangle$ of Eq. 9. It will be the same as the quantum Fisher information $F_q(\xi)$ attached to the probing state $|\widetilde{\psi}_\xi\rangle$ of Eq. 8 because of their unitary connection $|\psi_\xi\rangle = \mathsf{U}_\mathsf{F}^\dagger|\widetilde{\psi}_\xi\rangle$. From the probing state $|\widetilde{\psi}_\xi\rangle$ of Eq. 8, the differentiated state:

$$|\partial_\xi\widetilde{\psi}_\xi\rangle = i2\pi\sum_{k=0}^{N-1} k a_k \exp(i2\pi k\xi)|\bar{k}\rangle \tag{21}$$

leads to the inner products:

$$\langle\partial_\xi\widetilde{\psi}_\xi|\partial_\xi\widetilde{\psi}_\xi\rangle = 4\pi^2\sum_{k=0}^{N-1} k^2|a_k|^2 \tag{22}$$

and

$$\langle\partial_\xi\widetilde{\psi}_\xi|\widetilde{\psi}_\xi\rangle = -i2\pi\sum_{k=0}^{N-1} k|a_k|^2 \,. \tag{23}$$

The quantum Fisher information of Eq. 19 then follows as:

$$F_q(\xi) = 16\pi^2\left[\sum_{k=0}^{N-1} k^2|a_k|^2 - \left(\sum_{k=0}^{N-1} k|a_k|^2\right)^2\right] . \tag{24}$$

An interesting property revealed by Eq. 24 is that, for the parametric dependence achieved by the probing state $|\widetilde{\psi}_\xi\rangle$ of Eq. 8 with the phase ξ, the resulting quantum Fisher information $F_q(\xi)$ is found independent of the unknown phase ξ. This is an interesting property, not necessarily granted for all parametric dependence of a quantum state, and which ensures here that the ultimate estimation performance assessed by $F_q(\xi)$ stays the same for any range of the phase ξ to be estimated.

When the coefficients a_k of the input superposition are chosen according to Eq. 14 so as to minimize the estimation error $e^2(\widehat{\xi})$ as in Eq. 16, then the quantum Fisher information of Eq. 24 can be evaluated to be:

$$F_q(\xi) = 4\pi^2\left[\frac{1}{3}N^2 + \frac{2}{3} - \frac{2}{\sin^2(\pi/N)}\right] , \tag{25}$$

which at large N goes to $F_q(\xi) \to (4\pi^2/3 - 8)N^2 \approx 5.16N^2$. At large N, the analytical asymptotics $F_q(\xi) \sim N^2$ in Eq. 25 and $1/e^2(\widehat{\xi}) \sim N^2$ from Eq. 16, consistently match the evolution as $\sim N^2$ numerically observed for

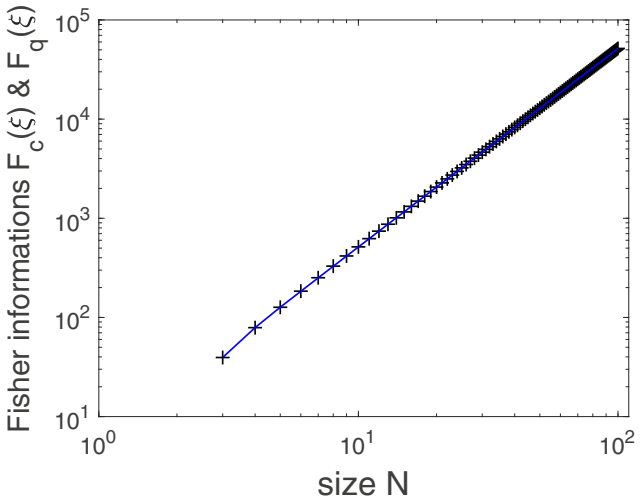

Fig. 7 Quantum Fisher information $F_q(\xi)$ of Eq. 25 (solid line), and classical Fisher information $F_c(\xi)$ from Eq. 18 (+) in the conditions of Fig. 5

$F_c(\xi)$ of Eq. 18 in Fig. 5. In addition, for any size N, the quantum Fisher information $F_q(\xi)$ of Eq. 25 is compared in Fig. 7 with the classical Fisher information $F_c(\xi)$ from Eq. 18 with the same optimal coefficients a_k of Eq. 14.

Figure 7 shows a classical Fisher information $F_c(\xi)$ which precisely matches the corresponding quantum Fisher information $F_q(\xi)$ of Eq. 25 attached to $|\psi_\xi\rangle$ and $|\widetilde{\psi}_\xi\rangle$, and in this respect saturates the inequality of Eq. 20. This indicates that no other measurement (be it generalized) of $|\psi_\xi\rangle$ of Eqs. 9 and 14–15, other than the measurement in the basis $\{|\overline{k}\rangle\}$, could reach a higher classical Fisher information $F_c(\xi)$; and no other processing of $|\widetilde{\psi}_\xi\rangle$ of Eqs. 8 and 14–15, other than the inverse Fourier transform followed by measurement in the basis $\{|\overline{k}\rangle\}$ as in Fig. 3, could reach a higher classical Fisher information $F_c(\xi)$. This applies with the excitation signal $|\psi_{\text{in}}\rangle$ of Eq. 7 optimized via Eq. 14. In these conditions, on the resulting probing signal $|\widetilde{\psi}_\xi\rangle$ of Eqs. 8 and 14–15, the processing of Fig. 3 consisting in the inverse Fourier transform to produce the signal $|\psi_\xi\rangle = \mathsf{U}_{\mathsf{F}}^{\dagger}|\widetilde{\psi}_\xi\rangle$ of Eq. 9 that is subsequently measured in the orthonormal basis $\{|\overline{k}\rangle\}$, stands as an essentially optimal processing of this $|\widetilde{\psi}_\xi\rangle$ for estimating the phase ξ. No other processing of the probing signal $|\widetilde{\psi}_\xi\rangle$ of Eqs. 8 and 14–15 could reach a larger classical Fisher information $F_c(\xi)$ and a more efficient estimation.

The optimization performed via Eq. 14 is practically meaningful because it uses as the optimization criterion the mean-squared error of a definite practical estimator, which is then minimized. This is a similar approach which is followed in [19] for quantum phase estimation, although on a different probing signal, as we indicated earlier. Our approach here consistently characterizes a complete strategy for quantum phase estimation, depicted in Fig. 3, including the definition of a probing signal, its Fourier-based processing and measurement followed by a definite estimator from the measurement results, together with an evaluation and optimization of the performance according to a criterion of minimal mean-squared error. One could nevertheless think of another approach for devising an efficient strategy of phase estimation, based on the optimization of a different criterion with a different meaning. We now describe such an alternative approach to devising an efficient strategy of phase estimation.

7 Direct maximum likelihood estimation

As an alternative approach, from the explicit expression we obtain for $F_q(\xi)$ in Eq. 24, one could seek the optimal coefficients a_k to place in the input excitation signal $|\psi_{\text{in}}\rangle$ of Eq. 7, in order to maximize the quantum Fisher information $F_q(\xi)$ in Eq. 24 (instead of minimizing the mean-squared estimation error as performed with Eq. 14). This represents a constrained (by the normalization of the a_k's) maximization of $F_q(\xi)$ in Eq. 24, that we solve by the Lagrange multiplier method in the Appendix. We then find in the Appendix that the maximal quantum Fisher information $F_q(\xi)$ in Eq. 24 is achieved by the coefficients $a_0 = a_{N-1} = 1/\sqrt{2}$ and $a_k = 0$ for $k = 1$ to $N-2$. This is associated in Eq. 7 with the $(N-1)$-qubit optimal excitation signal $|\psi_{\text{in}}\rangle = \big(|\overline{0}\rangle + |\overline{N-1}\rangle\big)/\sqrt{2} = \big(|0\cdots0\rangle + |1\cdots1\rangle\big)/\sqrt{2}$. Such an optimal signal is comparable to photonic NOON states as an extreme way of populating optical modes with photons [3, 4, 20]. At the optimum, the quantum Fisher information of Eq. 24 gets maximized at

$$F_q(\xi) = 4\pi^2(N-1)^2\,, \tag{26}$$

which at large N goes to $F_q(\xi) \to 4\pi^2N^2 \approx 39.48N^2$. It can be observed that the quantum Fisher information $F_q(\xi)$ of Eq. 26 is strictly larger than that of Eq. 25 for any size $N \geq 2$. However, it remains to be known whether, and how, the estimation performance associated with $F_q(\xi)$ of Eq. 26 can actually be achieved by an effective estimation strategy. It can, yet in a slightly restrictive way, as we now show.

The $(N-1)$-qubit optimal excitation signal:

$$|\psi_{\text{in}}\rangle = \frac{1}{\sqrt{2}}\Big(|\overline{0}\rangle + |\overline{N-1}\rangle\Big) \in \mathcal{H}'_N \tag{27}$$

achieving the maximal $F_q(\xi)$ of Eq. 26, induces in the setting of Fig. 3 the probing signal:

$$|\widetilde{\psi}_\xi\rangle = \mathsf{U}_\xi^{\otimes(N-1)}|\psi_{\text{in}}\rangle = \frac{1}{\sqrt{2}}\Big(|\overline{0}\rangle + \exp[i2\pi(N-1)\xi]|\overline{N-1}\rangle\Big)\,. \tag{28}$$

A direct measurement of the ξ-dependent probing signal $|\widetilde{\psi}_\xi\rangle \in \mathcal{H}'_N$ of Eq. 28 can be envisaged to estimate the

phase ξ. A projective measurement in the Hilbert space $\mathcal{H}'_N$ can be conceived, with one of the projective vectors of $\mathcal{H}'_N$ formed by the input state $|\psi_{\text{in}}\rangle \in \mathcal{H}'_N$ of Eq. 27. From the inner product $\langle\psi_{\text{in}}|\widetilde{\psi}_\xi\rangle = \big(1+\exp[i2\pi(N-1)\xi]\big)/2$, the probability in the measurement of projecting $|\widetilde{\psi}_\xi\rangle$ on $|\psi_{\text{in}}\rangle$ is:

$$P_0 = \big|\langle\psi_{\text{in}}|\widetilde{\psi}_\xi\rangle\big|^2 = \frac{1}{4}\big|1+\exp[i2\pi(N-1)\xi]\big|^2 \tag{29}$$

$$= \frac{1}{2}+\frac{1}{2}\cos[2\pi(N-1)\xi] \tag{30}$$

$$= \cos^2[\pi(N-1)\xi]\,. \tag{31}$$

It is enough to complement the quantum measurement in $\mathcal{H}'_N$ by a single additional projector projecting on the subspace of $\mathcal{H}'_N$ orthogonal to $|\psi_{\text{in}}\rangle$. This forms a valid quantum measurement for $|\widetilde{\psi}_\xi\rangle$, with only two orthogonal projectors to span $\mathcal{H}'_N$, yielding two possible outcomes, either $|\widetilde{\psi}_\xi\rangle$ is projected on $|\psi_{\text{in}}\rangle$ with the probability P_0 of Eq. 31, or $|\widetilde{\psi}_\xi\rangle$ is projected on the orthogonal subspace with the complementary probability $1-P_0$.

According to Eq. 17, such a two-outcome measurement is associated with the classical Fisher information:

$$F_c(\xi) = \frac{1}{P_0}\big(\partial_\xi P_0\big)^2 + \frac{1}{1-P_0}\big(\partial_\xi(1-P_0)\big)^2\,. \tag{32}$$

With P_0 from Eqs. 30 and 31 and some elementary trigonometric identities, for Eq. 32, one finally finds:

$$F_c(\xi) = 4\pi^2(N-1)^2\,. \tag{33}$$

So the two-outcome measurement reaches a classical Fisher information $F_c(\xi)$ in Eq. 33 that exactly matches the quantum Fisher information $F_q(\xi)$ of Eq. 26, which is itself maximized over all feasible excitation signals $|\psi_{\text{in}}\rangle$ in Eq. 7. No other estimation protocol can be expected to reach a higher efficiency in terms of the performance assessed by the Fisher information, classical and quantum. In practice, the maximum likelihood estimator directly applied on data delivered by the two-outcome measurement is assured to reach the performance dictated by the (classical) Fisher information, at least asymptotically in the limit of a large data record. This looks like a protocol with a performance strictly superior to that of the alternative Fourier-based estimation protocol of Section 4, so why bother with it in the first place ?

The reason is that the probing signal $|\widetilde{\psi}_\xi\rangle$ of Eq. 28, on which is grounded the estimation with superior Fisher information, probes the unknown phase ξ only through the multiple $(N-1)\xi$ (performing what is known as parameter amplification [19]), and the two-outcome measurement has a probability distribution $(P_0, 1-P_0)$ related to the unknown phase ξ only through the cosine of the amplified angle $2\pi(N-1)\xi$ as visible in Eq. 30. The consequence is that the data from the two-outcome measurement allow one to estimate (first) an amplified angle $2\pi(N-1)\xi \in [-\pi/2, \pi/2]$. This leads for the angle $2\pi\xi$ to multiple possible determinations $2\pi\xi \in [-\pi/2, \pi/2]/(N-1) + \pi n/(N-1)$ with integer $n \in [0, N-2]$. So for the phase ξ there are $N-1$ feasible determinations that cannot be distinguished from the measured data. This ambiguity can be lifted only with prior or additional information limiting the unknown phase ξ to one specific determination. In this respect, this estimation protocol performing parameter amplification realizes a local estimation, when one seeks to estimate, with a high accuracy, a very small change around a priorly known phase.

By contrast, the Fourier-based estimation, via the probing signal $|\widetilde{\psi}_\xi\rangle$ of Eq. 8, simultaneously probes a whole range of multiples $k\xi$, with $k = 0$ to $N-1$, of the unknown phase ξ. Consistently, the measurement of $|\psi_\xi\rangle = \mathsf{U}_{\mathsf{F}}^\dagger|\widetilde{\psi}_\xi\rangle$ of Eq. 9 with its N possible outcomes is able to extract, from $|\psi_\xi\rangle$, this richer information for estimating ξ. The associated estimator $\widehat{\xi} = j/N$ returns an estimate over the whole range $[0, 1[$ for ξ, with no ambiguity from multiple determinations. In this respect, the Fourier-based estimation protocol realizes a global estimation, over the whole feasible range of the unknown phase.

So both approaches, local and global, to quantum phase estimation offer complementary properties. Both approaches benefit from the favorable Heisenberg mean-squared error decreasing as $1/N^2$. The local approach assessed by Eq. 26 is the most accurate, with an rms error decreasing as $1/(2\pi N) \approx 0.16/N$, yet only to estimate a local change around a priorly known phase. The global Fourier-based approach assessed by Eq. 25 is a bit less accurate, with an rms error decreasing as $1/(\sqrt{4\pi^2/3-8}\,N) \approx 0.44/N$, but for estimation over the whole feasible range of the unknown phase. Still other phase estimation techniques have been proposed, offering other trade-offs, for lifting the ambiguity of multiple phase determinations, while also preserving the Heisenberg enhanced efficiency. For instance, adaptive techniques have been proposed to progressively adapt the measurement via successive estimates, or techniques varying among several excitation signals or measurements according to predefined schedules, or techniques employing more than one copy of the phase gate to be estimated [18–21, 32].

In the setting of the present study, for global quantum phase estimation, our approach offers a complete Fourier-based strategy with an evaluation of its performance optimized according to a criterion of minimal mean-squared error of a definite estimator. Strictly speaking, the results reported here do not exclude that there may still exist other alternative strategies for global phase estimation, with possibly superior performance according to some definite criterion. Other alternative strategies possibly probing the ξ-dependent process U_ξ in a different way, with an excitation signal other than $|\psi_{\text{in}}\rangle$ of Eqs. 7 and 14, experiencing

a processing other than the Fourier-based one used here, followed by a (possibly generalized) measurement other than measuring in the basis $\{|\overline{k}\rangle\}$, with the measurement results feeding another estimator, and preferably with some theoretical control on the functioning and performance, are yet to be proposed.

The Fourier-based approach is specifically useful since it involves a single measurement on a multiple-qubit signal to deliver a "one-shot" global phase estimate, with a precision that in principle can be made arbitrary high by increasing the size N of the probing signal. In its variant presented here, the Fourier-based approach, by using an optimally entangled probing signal, benefits from the Heisenberg enhanced efficiency with a mean-squared estimation error scaling as $1/N^2$. Moreover, it possesses the simplifying features for its physical implementation of requiring a single copy of the phase gate to be estimated, and of involving a multiple-qubit probing signal where each qubit (although entangled to the others) can be applied and measured separately.

8 Discussion

The variant of the Fourier-based approach, although presented here for estimating the phase induced by a qubit process U_ξ as in [22], could as well be adapted to phase estimation on an arbitrary quantum process U_ξ (not necessarily a qubit process). This would demand, as in [23], to use a controlled version of the arbitrary quantum process U_ξ (see for instance [9] and its Section 4.3 for this notion of controlled quantum process), with the possibility of arranging the control by qubits that would undergo the same transformation process as in Section 4.

As a complement to the studies of [22, 23] that examine the same Fourier-based method, the present analysis here extends the characterization with an assessment of the estimation performance, especially via the explicit evaluations of the Fisher information, both classical and quantum. This allowed us here to obtain a characterization of the overall best performance for estimation. The results analyze the conditions where, to realize a global phase estimation via a probing signal as $|\widetilde{\psi}_\xi\rangle$ in Eq. 8 probing a whole range of multiples $k\xi$ of the unknown phase, the Fourier-based processing described in Section 4 is optimal, and achieves the best estimation efficiency based on $|\widetilde{\psi}_\xi\rangle$. We note that with the present Fourier-based estimation scheme, the excitation signal $|\psi_{\text{in}}\rangle$ of Eq. 7 is an $(N-1)$-qubit state belonging to the N-dimensional subspace $\mathcal{H}'_N$, and it is enough to probe all the N multiples $k\xi$ of the unknown phase ξ, for $k = 0$ to $N-1$; using a higher-dimensional state belonging to the whole 2^{N-1}-dimensional space $\mathcal{H}_2^{\otimes(N-1)}$ of the $N-1$ qubits would, according to the numbers of qubits in state $|1\rangle$, redundantly probe the same multiples $k\xi$ and would add no extra capabilities not already accessible from the minimum-sized $|\psi_{\text{in}}\rangle$ of Eq. 7.

Quantum phase estimation, as addressed here, is at the root of many practical applications, as sketched in the "Introduction", and connects to many directions still open for exploration [33, 34]. It connects to general or multiparametric quantum system identification, also known as quantum process tomography, which especially can be assessed with the same concept of Fisher information, classical and quantum, exploited here. For telecommunications [35–37], this relates for instance to the tasks of quantum channel estimation and equalization, quantum system inversion related to quantum source separation [38].

One specially interesting direction for further exploration would be to analyze the evolution of the estimation performance in the presence of quantum noise. Quantum noise or decoherence represents the alteration of quantum states caused by their interaction with an uncontrolled environment [7, 9, 39–42]. Quantum noise is a ubiquitous factor generally impacting the performance of quantum processing and quantum technologies. In the course of elaborating methodologies for quantum information and signal processing, it is therefore relevant to come to examine how their performance evolves in the presence of quantum noise. For Fourier-based quantum phase estimation, few studies have examined the impact of quantum noise, following different noise models [19, 21–23, 43]. Specifically, [22, 23] considered the impact of quantum phase noise—which is specially relevant when phase information is to be retrieved—taken into account at the level of each probing qubit under the form of a nonunitary evolution [9, 42], and when the quantum states are treated as mixed states [9] expressible as convex combinations (convex sums) of pure states setting the reference in the present study. As a complement to [22, 23], one could examine the impact of the phase noise on the classical and quantum Fisher information of Sections 5 and 6 to establish the ultimate efficiency for phase estimation in the presence of noise, and how practical approaches stand in relation to such limits.

For estimation with quantum noise, one could also investigate the existence of special regimes of stochastic resonance, where the presence of noise is not necessarily detrimental but can prove beneficial to improve the performance. Such noise-enhanced performance has been widely explored for classical signal processing [44–51]. Recently, concerning quantum signal processing, some regimes of stochastic resonance have been observed in the quantum [52] and classical [53] Fisher information in the presence of quantum noise. It could be interesting to investigate if regimes of enhancement by quantum noise

could be observed in the performance of the Fourier-based phase estimation approaches considered here.

Beyond its significance to quantum phase estimation, the present study illustrates how the standard conceptualizations and methodologies of signal processing naturally find their way at the quantum level, and can thus take part in the ongoing developments of quantum information processing and quantum technologies. Much remains to be accomplished in these areas, and the thread of quantum signal processing constitutes a useful contribution to this science endeavor.

Appendix

The constrained maximization of the quantum Fisher information $F_q(\xi)$ in Eq. 24 can be approached in the N real variables $x_k = |a_k|$. Accordingly, in the variables x_k, we consider the constrained maximization associated with the Lagrange multiplier μ and Lagrangian:

$$\mathcal{L} = \sum_{k=0}^{N-1} k^2 x_k^2 - \left(\sum_{k=0}^{N-1} k x_k^2 \right)^2 + \mu \left(\sum_{k=0}^{N-1} x_k^2 - 1 \right) . \quad (34)$$

In particular, the form of the Lagrangian $\mathcal{L}$ which depends only on the squared variables x_k^2 renders unnecessary to additionally enforce that the variables x_k should be positive. By differentiation, we obtain the necessary condition for extremality as the system of $N + 1$ equations:

$$\begin{cases} \dfrac{\partial \mathcal{L}}{\partial x_k} = 2k^2 x_k - 4k x_k \left(\sum\limits_{\ell=0}^{N-1} \ell x_\ell^2 \right) + 2\mu x_k = 0 , & (35) \\ \dfrac{\partial \mathcal{L}}{\partial \mu} = \sum\limits_{\ell=0}^{N-1} x_\ell^2 - 1 = 0 , & (36) \end{cases}$$

for all $k = 0$ to $N - 1$.

A solution to the system of Eqs. 35 and 36 exists with a single nonzero $x_k = 1$, feasible for any $k = 0$ to $N - 1$, and $\mu = k^2$, which gives a vanishing Fisher information $F_q(\xi) = 0$ in Eq. 24. This corresponds to a minimum of the non-negative Fisher information $F_q(\xi)$.

Another solution to the system of Eqs. 35 and 36 exists with only two nonzero x_{k_1} and x_{k_2} for some $k_1 \neq k_2$. From Eqs. 35 and 36, it follows that $x_{k_1}^2 = x_{k_2}^2 = 1/2$ and $\mu = k_1 k_2$. This is a necessary condition for the extremization of the Fisher information $F_q(\xi)$, which applies for any pair of k_1 and $k_2 \neq k_1$, and realizes in Eq. 24 the Fisher information $F_q(\xi) = 4\pi^2 (k_2 - k_1)^2$ which is maximized at $F_q(\xi) = 4\pi^2 (N-1)^2$ when $k_1 = 0$ and $k_2 = N - 1$.

Beyond, when three or more x_k's are nonzero, it can be verified that no solution exists to the system of Eqs. 35 and 36.

References

1. Acín A et al (2018) The quantum technologies roadmap: a European community view. New J Phys 20:080201,1–24
2. Gisin N, Thew RT (2010) Quantum communication technology. Electron Lett 46:965–967
3. Giovannetti V, Lloyd S, Maccone L (2011) Advances in quantum metrology. Nat Photonics 5:222–229
4. Degen CL, Reinhard F, Cappellaro P (2017) Quantum sensing. Rev Mod Phys 89:035002,1–39
5. Tan X, Zhou X (2017) Universal half-blind quantum computation. Ann Telecommun 72:589–595
6. Nguyen HV, Babar Z, Alanis D, Botsinis P, Chandra MA, Mohd Izhar D, Ng SX, Hanzo L (2017) Towards the quantum internet: Generalised quantum network coding for large-scale quantum communication networks. IEEE Access 5:17288–17308
7. Preskill J (2018) Quantum computing in the NISQ era and beyond. Quantum 2:79,1–20
8. Zhou S, Zhang M, Preskill J, Jiang L (2018) Achieving the Heisenberg limit in quantum metrology using quantum error correction. Nat Commun 9:78,1–11
9. Nielsen MA, Chuang IL (2000) Quantum computation and quantum information. Cambridge, Cambridge University Press
10. Botsinis P, Alanis D, Babar Z, Nguyen H, Chandra D, Ng SX, Hanzo L (2019) Quantum search algorithms for wireless communications. IEEE Commun Surveys Tutorials 21:1209–1242
11. Giovannetti V, Lloyd S, Maccone L (2004) Quantum-enhanced measurements: Beating the standard quantum limit. Science 306:1330–1336
12. Huelga SF, Macchiavello C, Pellizzari T, Ekert AK, Plenio MB, Cirac JI (1997) Improvement of frequency standards with quantum entanglement. Phys Rev Lett 79:3865–3868
13. Shor PW (1997) Polynomial-time algorithms for prime factorization and discrete logarithms on a quantum computer. SIAM J Comput 26:1484–1509
14. Abbott BP et al (2016) Observation of gravitational waves from a binary black hole merger. Phys Rev Lett 116:061102,1–16
15. Kitaev A (1995) Quantum measurements and the Abelian stabilizer problem. arXiv:quant-ph/9511026 (22 pages)
16. Cleve R, Ekert A, Macchiavello C, Mosca M (1998) Quantum algorithms revisited. Proc R Soc Lond A 454:339–354
17. Chappell JM, Lohe MA, von Smekal L, Iqbal A, Abbott D (2011) A precise error bound for quantum phase estimation. Plos One 6:e19663,1–4
18. van Dam W, D'Ariano GM, Ekert A, Macchiavello C, Mosca M (2007) Optimal quantum circuits for general phase estimation. Phys Rev Lett 98:090501,1–4
19. Ji Z, Wang G, Duan R, Feng Y, Ying M (2008) Parameter estimation of quantum channels. IEEE Trans Inf Theory 54:5172–5185
20. Berry DW, Higgins BL, Bartlett SD, Mitchell MW, Pryde GJ, Wiseman HM (2009) How to perform the most accurate possible phase measurements. Phys Rev A 80:052114,1–22
21. Kaftal T, Demkowicz-Dobrzański R (2014) Usefulness of an enhanced Kitaev phase-estimation algorithm in quantum metrology and computation. Phys Rev A 90:062313,1–6
22. Chapeau-Blondeau F, Belin E (2019) Transformée de Fourier et traitement du signal quantique. In: Proceedings 27è Colloque GRETSI sur le Traitement du Signal et des Images, Lille, France, pp 26–29
23. Chapeau-Blondeau F, Belin E (2020) Fourier-transform quantum phase estimation with quantum phase noise. Signal Process 170:107441,1–10
24. Giovannetti V, Lloyd S, Maccone L (2006) Quantum metrology. Phys Rev Lett 96:010401,1–4

25. Zwierz M, Prez-Delgado CA, Kok P (2010) General optimality of the Heisenberg limit for quantum metrology. Phys Rev Lett 105:180402,1–4
26. Cover TM, Thomas JA (1991) Elements of information theory. Wiley, New York
27. Kay SM (1993) Fundamentals of statistical signal processing: estimation theory. Prentice Hall, Englewood Cliffs
28. Braunstein SL, Caves CM (1994) Statistical distance and the geometry of quantum states. Phys Rev Lett 72:3439–3443
29. Barndorff-Nielsen OE, Gill RD (2000) Fisher information in quantum statistics. J Phys A 33:4481–4490
30. Paris MGA (2009) Quantum estimation for quantum technology. Int J Quant Inform 7:125–137
31. Chapeau-Blondeau F (2015) Optimized probing states for qubit phase estimation with general quantum noise. Phys Rev A 91:052310,1–13
32. Berry DW, Wiseman HM (2000) Optimal states and almost optimal adaptive measurements for quantum interferometry. Phys Rev Lett 85:5098–5101
33. Simon DS, Jaeger G, Sergienko AV (2017) Quantum metrology, imaging, and communication. Springer, Berlin
34. Jones JA, Jaksch D (2012) Quantum information, computation and communication. Cambridge, Cambridge University Press
35. Imre S, Gyongyosi L (2012) Advanced quantum communications: an engineering approach. Wiley-IEEE Press, New York
36. Cariolaro G (2015) Quantum communications. Springer, Berlin
37. Benslama M, Benslama A, Aris S (2017) Quantum communications in new telecommunications systems. Wiley-ISTE, London
38. Deville Y, Deville A (2012) Classical-processing and quantum-processing signal separation methods for qubit uncoupling. Quantum Inf Process 11:1311–1347
39. Abram I (1996) Quantum noise of optical oscillators and amplifiers. Annales Des Télécommunications 51:361–372
40. Shaji A, Caves CM (2007) Qubit metrology and decoherence. Phys Rev A 76:032111,1–13
41. Kappe P, Kaiser J, Elsässer W, Wirth R, Streubel K (2003) Investigations of the fundamental quantum noise properties of resonant-cavity light-emitting diodes (RCLEDs). Annales Des Télécommunications 58:1424–1431
42. Chapeau-Blondeau F (2015) Optimization of quantum states for signaling across an arbitrary qubit noise channel with minimum-error detection. IEEE Trans Inf Theory 61:4500–4510
43. O'Brien TE, Tarasinski B, Terhal BM (2019) Quantum phase estimation of multiple eigenvalues for small-scale (noisy) experiments. New J Phys 21:023022,1–28
44. Luchinsky DG, Mannella R, McClintock PVE, Stocks NG (1999) Stochastic resonance in electrical circuits – I: Conventional stochastic resonance. IEEE Transactions on Circuits and Systems – II: Analog and Digital Signal Processing 46:1205–1214
45. Zozor S, Amblard PO (2003) Stochastic resonance in locally optimal detectors. IEEE Trans Signal Process 51:3177–3181
46. Duan F, Chapeau-Blondeau F, Abbott D (2006) Noise-enhanced SNR gain in parallel array of bistable oscillators. Electron Lett 42:1008–1009
47. Fiorina J, Rousseau D, Chapeau-Blondeau F (2006) Interferer rejection improved by noise in ultra-wideband telecommunications. Fluctuation and Noise Letters 6:L317–L328
48. Chen H, Varshney PK, Michels JH (2008) Noise enhanced parameter estimation. IEEE Trans Signal Process 56:5074–5081
49. Patel A, Kosko B (2010) Optimal mean-square noise benefits in quantizer-array linear estimation. IEEE Signal Processing Letters 17:1005–1009
50. Bayram S, Gezici S (2012) Stochastic resonance in binary composite hypothesis-testing problems in the Neyman-Pearson framework. Digital Signal Processing 22:391–406
51. Duan F, Chapeau-Blondeau F, Abbott D (2013) Weak signal detection: Condition for noise induced enhancement. Digital Signal Processing 23:1585–1591
52. Chapeau-Blondeau F (2015) Qubit state estimation and enhancement by quantum thermal noise. Electron Lett 51:1673–1675
53. Gillard N, Belin E, Chapeau-Blondeau F (2019) Stochastic resonance with unital quantum noise. Fluctuation and Noise Letters 18:1950015,1–15